



# Simultaneous removal of NO<sub>x</sub> and soot particulates over La<sub>0.7</sub>Ag<sub>0.3</sub>MnO<sub>3</sub> perovskite oxide catalysts

Ke Wang, Ling Qian, Lei Zhang, Huanrong Liu, Zifeng Yan\*

State Key Laboratory of Heavy Oil Processing, CNPC Key Laboratory of Catalysis, College of Chemistry and Chemical Engineering, China University of Petroleum, Qingdao 266555, China

## ARTICLE INFO

### Article history:

Available online 3 July 2010

### Keywords:

La<sub>0.7</sub>Ag<sub>0.3</sub>MnO<sub>3</sub> catalyst  
Simultaneous removal of NO<sub>x</sub> and diesel soot  
Solid state method

## ABSTRACT

A highly active catalyst (La<sub>0.7</sub>Ag<sub>0.3</sub>MnO<sub>3</sub>) for simultaneous removal of nitrogen oxides (NO<sub>x</sub>) and diesel soot is synthesized by solid state method and the catalyst is characterized by XRD, FT-IR, H<sub>2</sub>-TPR, and O<sub>2</sub>-TPD. The results indicate that metallic Ag appears in the La<sub>0.7</sub>Ag<sub>0.3</sub>MnO<sub>3</sub> catalyst. The concentration of oxygen vacancy and the over-stoichiometry oxygen content also remarkably increase as the substitution increase of Ag<sup>+</sup> for La<sup>3+</sup> at A-site ions. The simultaneous removal of soot particulates and NO<sub>x</sub> activities are evaluated by a temperature-programmed reaction (TPRe) technique. The superior performance of the La<sub>0.7</sub>Ag<sub>0.3</sub>MnO<sub>3</sub> catalyst for the reaction is probably due to lots of oxygen vacancy and over-stoichiometry oxygen in the perovskite lattice along with the zero-valence silver.

© 2010 Elsevier B.V. All rights reserved.

## 1. Introduction

Perovskite-structured (ABO<sub>3</sub>) oxides, as a potential catalyst for simultaneous removal of soot particulates and NO<sub>x</sub> in diesel exhaust, have been investigated widely in academic and industry after the proposal of a catalyzed soot traps process [1]. The partial replacement of the A-site ions by alkali metal [2,3,4], alkali-earth metal [4] and rare-earth metal [5] in perovskite-structure will lead to structural defects in the crystal lattice, which might enhance the activity and selectivity for simultaneous removal of NO<sub>x</sub> and soot. Silver could not only increase the carbon gasification rate [6], but also shows remarkable performances in NO<sub>x</sub> abatement [7,8]. Silver supported alumina catalyst has also shown good performance on simultaneous removal of carbon particle and NO<sub>x</sub> [9]. It is therefore possible to develop highly effective simultaneous removal of NO<sub>x</sub> and soot catalysts by using Ag<sup>+</sup> replaced A-site ions of perovskite oxides.

Herein, we partially replaced La<sup>3+</sup> ions of LaMnO<sub>3</sub> perovskite oxide by Ag<sup>+</sup> ions, and La<sub>0.7</sub>Ag<sub>0.3</sub>MnO<sub>3</sub> with prescribed stoichiometry was used as a catalyst for simultaneous removal of NO<sub>x</sub> and soot. The results indicated that the structural defects produced by Ag<sup>+</sup> ions replacement in the crystal lattice will affect the catalytic activity. Meanwhile, metallic silver in this catalyst might also promote the performance for simultaneous removal of NO<sub>x</sub> and soot.

## 2. Experimental

### 2.1. Catalyst preparation

The La(NO<sub>3</sub>)<sub>3</sub>·6H<sub>2</sub>O, AgNO<sub>3</sub>·H<sub>2</sub>O and Mn(CH<sub>3</sub>COO)<sub>2</sub>·4H<sub>2</sub>O powders with a stoichiometric ratio were mixed and grinded continuously for 20 min in a mortar. Compared with the theoretical weight, 20% excessive NaOH was added into the mortar, and grinding the solid to react completely. Then the as-synthesized sample was washed with deionized water by filter. The solid product was dried at 100 °C for 24 h, followed by calcination at 600 °C for 10 h in air. After grinding, the catalyst powder (150–200 mesh) was obtained.

### 2.2. Catalyst characterization

Fourier transform infrared (FT-IR) spectra were recorded at room temperature from 4000 to 400 cm<sup>-1</sup> by a Nicolet 6700 spectrometer, and 64 scans were collected with a resolution of 2 cm<sup>-1</sup>. A self-supporting disk (10 mm diameter) prepared by pressing the mixture of sample powder and KBr was placed into a conventional metal cell with KBr windows.

The X-ray diffraction (XRD) patterns of the samples were measured on a powder X-ray diffractometer (PANalytical XRD Xpert pro. MPD) using Cu Kα radiation (λ = 0.1542 nm) in the 2θ range of 10–75° at a scanning rate of 2° per min. The tube voltage and current were set at 40 kV and 40 mA, respectively. The patterns were compared with JCPDS reference data for phase identification.

H<sub>2</sub>-TPR measurements were carried out on a Quantachrome ChemBET-3000. Typically, 100 mg sample was pretreated at a

\* Corresponding author. Tel.: +86 532 86981296/86981856; fax: +86 532 86981295.

E-mail address: [zfyan@upc.edu.cn](mailto:zfyan@upc.edu.cn) (Z. Yan).

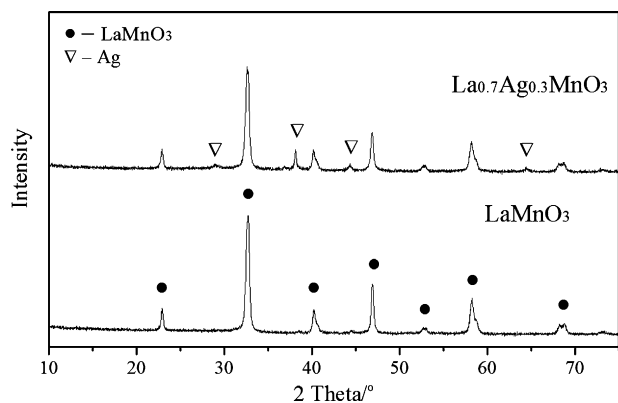


Fig. 1. X-ray diffraction patterns of catalysts.

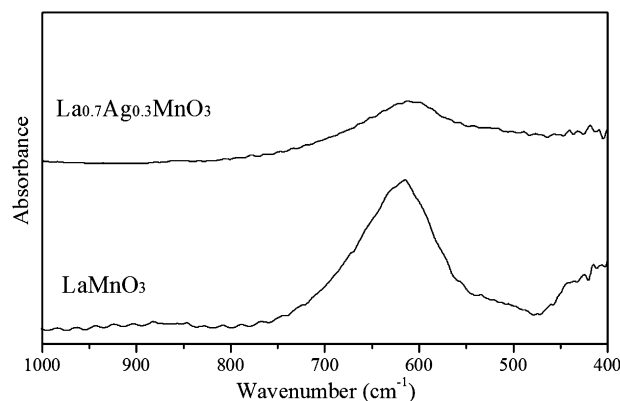


Fig. 2. FT-IR spectra of catalysts.

helium atmosphere at 500 °C for 1 h and subsequently cooled to 50 °C. Then, the H<sub>2</sub>-TPR was carried out using 9.87% hydrogen in argon at a constant flow rate of 70 mL/min, from 100 °C to 800 °C at a heating rate of 10 °C/min.

The O<sub>2</sub>-TPD experiments were performed on Quantachrome ChemBET-3000. 200 mg of the sample was pretreated using 4.16% O<sub>2</sub> in He (80 mL/min) at 600 °C for 30 min, and then cooled down to room temperature in the same atmosphere. The oxygen desorbed gradually from 100 °C to 850 °C at a heating rate of 10 °C/min in He stream.

### 2.3. Catalytic activity evaluation

The catalytic activities of the prepared samples were evaluated with a temperature-programmed reaction (TPRe) technique. The reaction temperature varied during each TPRe run from 200 °C to 600 °C at a 4 °C/min rate. The model soot particulates used was the Printex-U sample supplied by Degussa. 165 mg mixture of soot particulates and La<sub>0.7</sub>Ag<sub>0.3</sub>MnO<sub>3</sub> catalyst was carefully mixed, in the weight ratio of 1/10 for a “loose” contact between the soot particulates and the catalyst, and then placed into the center of a quartz reactor. The simulated exhaust consists of 0.2% NO, 5% O<sub>2</sub> with He as the major gas and the total flow rate is 60 mL/min. After reaction, the gas is automatically sampled and analyzed by a gas chromatograph (modified Agilent-6820 GC) equipped with a TCD and with a Porapak Q column for separating CO<sub>2</sub> and N<sub>2</sub>O, and a molecular sieve 5A column for separating O<sub>2</sub>, N<sub>2</sub> and CO. During the test of this work, N<sub>2</sub>O and CO was not detectable.

The catalytic activity was evaluated by the values of  $T_{10}$ ,  $T_{50}$ , and  $T_{90}$ , which were defined as the temperatures at which 10, 50, and 90% of the soot particulates were oxidized during the TPRe procedure, respectively. The maximum NO conversion into N<sub>2</sub> is another important parameter, which can be calculated by  $2[N_2]_o/[NO]_i$ , where  $[N_2]_o$  and  $[NO]_i$  are concentrations of N<sub>2</sub> in the outlet gas and NO in the inlet gas, respectively. In the TPRe experiments, the reaction was continuously run until the soot was completely burnt off.

## 3. Results and discussion

### 3.1. XRD

The X-ray diffraction patterns of La<sub>1-x</sub>Ag<sub>x</sub>MnO<sub>3</sub> ( $x=0, 0.3$ ) catalysts are shown in Fig. 1. It reveals that the LaMnO<sub>3</sub> catalyst is rhombohedral perovskite phase in the present work. For La<sub>0.7</sub>Ag<sub>0.3</sub>MnO<sub>3</sub> catalyst, four additional peaks not belonging to the perovskite phase are observed at 29.1°, 38.1°, 44.3° and 64.4°, and they can be assigned to metallic Ag.

### 3.2. FT-IR

IR spectrum of LaMnO<sub>3</sub> perovskite presents two strong absorption bands around 600–650 cm<sup>-1</sup> and ~400 cm<sup>-1</sup>, as shown in Fig. 2. Lavat and Baran [10] found that the BO<sub>6</sub> units dominate the spectroscopic behavior because, the B–O bonds of the BO<sub>6</sub> octahedral units are undoubtedly stronger than those of the 12-coordinated La(III)–O units. The bands in the range of 600–650 cm<sup>-1</sup> are assigned to the asymmetric stretching vibration of the BO<sub>6</sub> octahedra, while those at ~400 cm<sup>-1</sup> are ascribed to the deformation modes of the same polyhedral [11]. In the IR spectra of La<sub>0.7</sub>Ag<sub>0.3</sub>MnO<sub>3</sub> sample, the broadening of the bands at higher wave numbers and decreasing of their intensity, along with disappearing bands at lower wave numbers, were observed. It is plausible that BO<sub>6</sub> octahedral units in the structure of La<sub>0.7</sub>Ag<sub>0.3</sub>MnO<sub>3</sub> are more symmetric than that in LaMnO<sub>3</sub> because an amount of Ag<sup>+</sup> substitutes La<sup>3+</sup> at A-site getting into the lattice of perovskite oxide.

### 3.3. H<sub>2</sub>-TPR

Fig. 3 shows the H<sub>2</sub>-TPR patterns of La<sub>1-x</sub>Ag<sub>x</sub>MnO<sub>3</sub> ( $x=0, 0.3$ ) catalysts. In all cases, two types of chemisorbed oxygen species, were observed: a low-temperature species, named  $\alpha$ , desorbing below 600 °C, and a high-temperature one, named  $\beta$ , reacting in the region of 600–900 °C. The  $\alpha$  peak depends strongly on the concentration of surface oxygen vacancies. In particular, its onset and intensity depend partly on the nature of the metal B of ABO<sub>3</sub> structure, but principally on the degree of substitution of the A-site ions with cations with lower valence [12]. Otherwise, nonstoichiometric excess oxygen appears, which is mostly weakly bonded in the perovskite lattice [13], and impacts on the  $\alpha$  peak. A dramatic shift to low temperatures of the peak of  $\alpha$ -oxygen species and the incre-

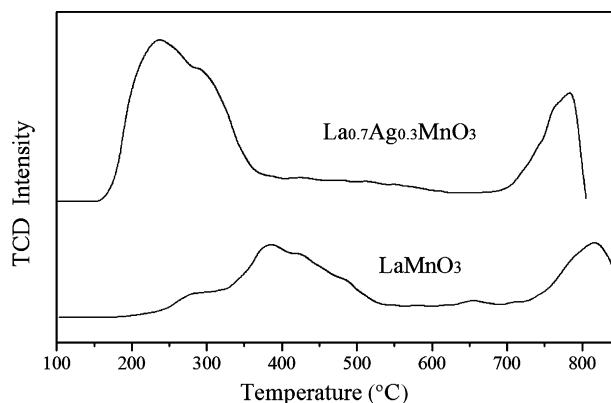


Fig. 3. The H<sub>2</sub>-TPR patterns of catalysts.

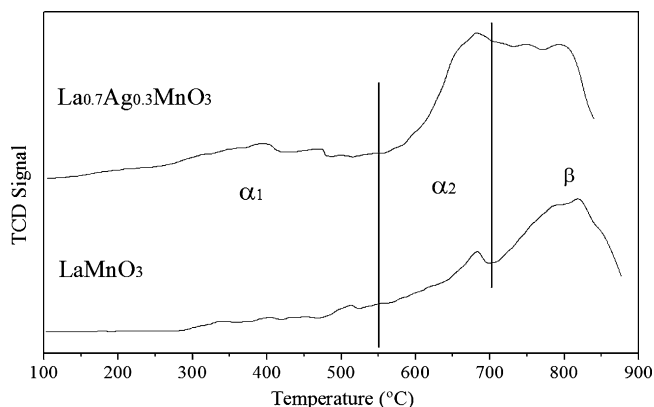
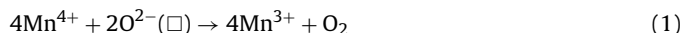


Fig. 4. The O<sub>2</sub>-TPD profiles of catalysts.

ment of its peak area were both observed when LaMnO<sub>3</sub> was doped with silver. It can be deduced that a large amount of oxygen vacancies producing in the structure of La<sub>0.7</sub>Ag<sub>0.3</sub>MnO<sub>3</sub>, as a result of the partial substitution of Ag<sup>+</sup> for La<sup>3+</sup> at A-site ions, affects strongly the oxygen mobility in the catalyst. Concerning high-temperature β-oxygen species, Spinicci and Tofanari [14] demonstrated that this peak could be referred to as the lattice oxygen. The LaMnO<sub>3</sub> shows β peak at 817 °C, while the corresponding peak shifts to 783 °C and becomes narrower for La<sub>0.7</sub>Ag<sub>0.3</sub>MnO<sub>3</sub>.

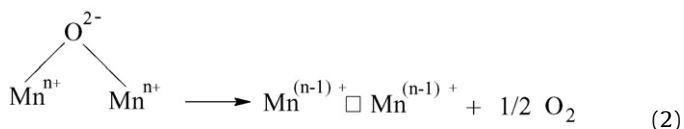
### 3.4. O<sub>2</sub>-TPD

In the O<sub>2</sub>-TPD patterns of catalysts (Fig. 4), two kinds of desorbed oxygen species, α-O<sub>2</sub> ( $T < 700$  °C) and β-O<sub>2</sub> ( $T > 750$  °C), were also observed. However, α-O<sub>2</sub> are divided into two subgroups [15] with the low temperature desorbing one being designated as α<sub>1</sub>-O<sub>2</sub> and the one desorbing above 550 °C as α<sub>2</sub>-O<sub>2</sub>. α<sub>1</sub>-O<sub>2</sub> is ascribed to O<sub>2</sub> adsorbed on anion vacancies (oxygen vacancies) which can be readily removed at relatively low temperature, while α<sub>2</sub>-O<sub>2</sub> is assigned to the desorption of over-stoichiometric oxygen (excess O<sub>2</sub>) at 600–700 °C which may be formulated as:



In Eq. (1) the excess oxygen charge is compensated by cation vacancies (noted here as (□)) following the suggestions of van Roosmalen et al. [16]. As shown in Fig. 4, the peak intensity of α<sub>1</sub>-O<sub>2</sub> and α<sub>2</sub>-O<sub>2</sub> of La<sub>0.7</sub>Ag<sub>0.3</sub>MnO<sub>3</sub> catalyst is stronger than that of LaMnO<sub>3</sub>, in agreement with the result of H<sub>2</sub>-TPR.

The desorption temperature of β-O<sub>2</sub> is at 819 °C for the LaMnO<sub>3</sub> and near 800 °C for the La<sub>0.7</sub>Ag<sub>0.3</sub>MnO<sub>3</sub> catalyst. The desorption temperature of β-oxygen species is often associated with the mobility in the bulk of the structure. This desorption requires the formation of the β-O<sub>2</sub> desorption site [17]:



where  $n=4$  or  $3$  and □ is an anion vacancy.

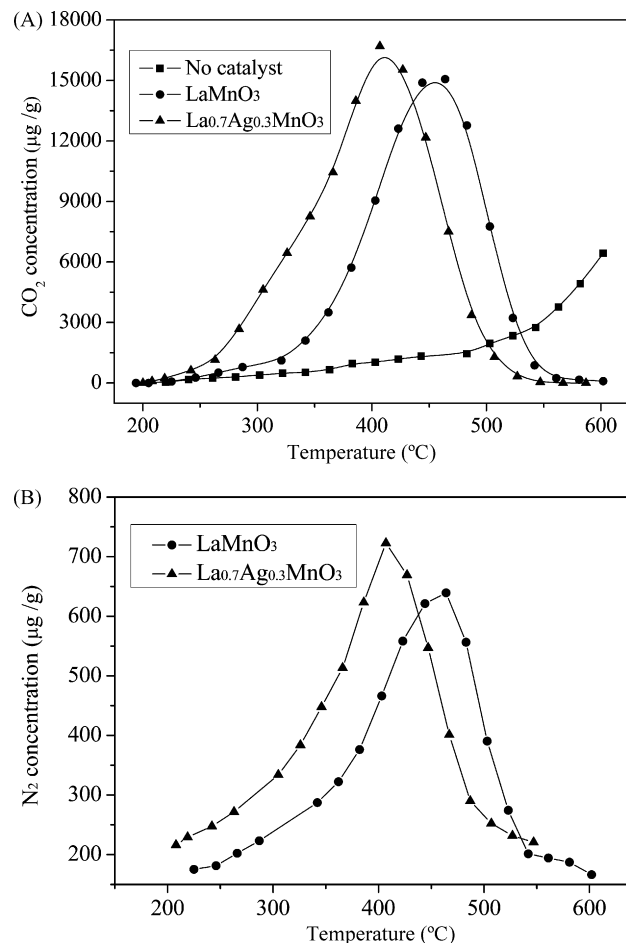
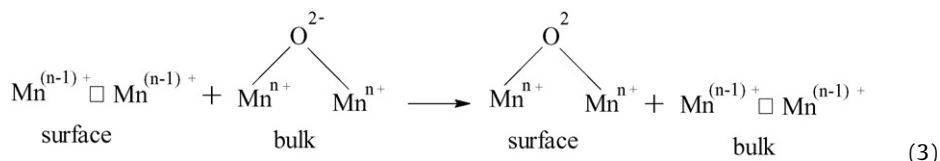


Fig. 5. The outlet CO<sub>2</sub> and N<sub>2</sub> concentration profiles during temperature-programmed reaction over La<sub>1-x</sub>Ag<sub>x</sub>MnO<sub>3</sub> ( $x=0, 0.3$ ) catalysts: (A) outlet CO<sub>2</sub> concentration profiles and (B) outlet N<sub>2</sub> concentration profiles.

Thereafter, β-oxygen desorption proceeds via the diffusion of oxygen from the bulk to the surface:



According to the temperature ranges of α and β peaks, it seems that α-oxygen species should be directly responsible for the soot particulates combustion.

### 3.5. Catalytic activity

Fig. 5 and Table 1 show the result of the TPRE over La<sub>1-x</sub>Ag<sub>x</sub>MnO<sub>3</sub> ( $x=0, 0.3$ ). It manifests that N<sub>2</sub> and CO<sub>2</sub> are produced over the catalysts at the same temperature range, which illuminates that the catalysts have the capability of simultaneous removal of NO<sub>x</sub> and soot particulates. In the present study, soot particulates in non-catalytic combustion cannot be consumed completely under the same reaction conditions, when the maximum of CO<sub>2</sub> concentration is only 6426 μg/g and N<sub>2</sub> is not detected. The catalysts decrease remarkably the temperature of soot particulates combustion. As shown in Fig. 5, LaMnO<sub>3</sub> exhibits a high catalytic activity for soot combustion and NO reduction. Compared to LaMnO<sub>3</sub>, the combustion temperature of soot particulates decreases more than 40 °C on La<sub>0.7</sub>Ag<sub>0.3</sub>MnO<sub>3</sub>, and

**Table 1**

The catalytic performances of  $\text{La}_{1-x}\text{Ag}_x\text{MnO}_3$  ( $x=0, 0.3$ ) catalysts for simultaneous removal of soot and NOx.

Sample	$T_{10}/^\circ\text{C}$	$T_{50}/^\circ\text{C}$	$T_{90}/^\circ\text{C}$	Maximum conversion of NO into $\text{N}_2/\%$
$\text{LaMnO}_3$	367	443	501	63.9
$\text{La}_{0.7}\text{Ag}_{0.3}\text{MnO}_3$	317	401	461	72.2

the maximum NO conversion into  $\text{N}_2$  increases from 63.9% to 72.2%.

The high activity for simultaneous removal of NOx and soot particulates of  $\text{La}_{0.7}\text{Ag}_{0.3}\text{MnO}_3$  catalyst might attribute to the following two factors. The first one is the increase in the content of oxygen vacancies and over-stoichiometric oxygen due to the partial substitution of  $\text{Ag}^+$  for  $\text{La}^{3+}$  at A-site ions.  $\text{O}_2$ -TPD results confirm that a mass of oxygen vacancies exist in the  $\text{La}_{0.7}\text{Ag}_{0.3}\text{MnO}_3$  catalyst. Using MS-NO-TPD method, Zhao and co-workers [18] investigated the relationship between oxygen vacancy and adsorption and activation of NO on the perovskite-like oxide catalysts. The result reveals that the adsorption of NO, which is strongly related to the oxygen vacancy concentration, is significant to the activation of NO molecule. The improvement of the mobility of oxygen caused by enhancement of over-stoichiometric oxygen content, promotes the contacts between oxygen and soot particulates. Therefore, it improves the catalytic activity for simultaneous removal of NOx and soot particulates. The second reason is that metallic Ag is presented in the catalyst, as confirmed by XRD.  $\text{NO}_2$  is much more reactive towards soot than NO and  $\text{O}_2$  as it was confirmed by literature [19,20,21], while Zhao and co-workers [22] postulated that, due to the strong oxidizing ability of  $\text{NO}_2$  and the good contact property of  $\text{NO}_2$  molecule with soot particles, the soot combustion rate was accelerated. Metallic Ag in  $\text{La}_{0.7}\text{Ag}_{0.3}\text{MnO}_3$  catalyst can efficiently adsorb NO and  $\text{O}_2$ , and oxidize NO to  $\text{NO}_2$  [23], causing that both soot oxidation rate and NOx reduction rate are enhanced.

#### 4. Conclusion

The  $\text{La}_{0.7}\text{Ag}_{0.3}\text{MnO}_3$  catalyst has good catalytic performance for simultaneous removal of NOx and diesel soot particulates under loose contact conditions. Several conclusions can be drawn from this work. The partial substitution of  $\text{Ag}^+$  for  $\text{La}^{3+}$  at A-site ions enhanced the catalytic activity due to the increase of oxygen vacancy concentration and the over-stoichiometry oxygen content. The oxygen vacancy is beneficial because it enhances the adsorption and activation of NO or molecular oxygen, while over-stoichiometry oxygen accelerates the mobility of oxygen in the catalyst. The existence of metallic Ag in the catalyst speeds up the combustion rate of soot particulates and also promotes the reduction rate of NO. The lower temperature of soot particulates combustion and the higher conversion of NO towards  $\text{N}_2$  are obtained as a result of the synergetic effect of those factors discussed.

#### Acknowledgement

The temperature-programmed reaction (TPRe) test from Professor Zhengping Hao' group in the Research Center for Eco-Environmental Sciences in Chinese Academy of Sciences was greatly appreciated.

#### References

- [1] K. Yoshida, S. Makino, S. Sumiya, G. Muramatsu, R. Helferich, SAE paper 1989-89-2046.
- [2] Y. Teraoka, K. Kanada, S. Kagawa, Synthesis of La–K–Mn–O perovskite-type oxides and their catalytic property for simultaneous removal of NOx and diesel soot particulates, *Appl. Catal. B* 34 (2001) 73–78.
- [3] N. Russo, D. Fino, G. Saracco, V. Specchia, Studies on the redox properties of chromite perovskite catalysts for soot combustion, *J. Catal.* 229 (2005) 459–469.
- [4] Y. Teraoka, K. Nakano, S. Kagawa, W.F. Shangguan, Simultaneous removal of nitrogen oxides and diesel soot particulates catalyzed by perovskite-type oxides, *Appl. Catal. B* 5 (1995) L181–L185.
- [5] S.S. Hong, G.D. Lee, Simultaneous removal of NO and carbon particulates over lanthanoid perovskite-type catalysts, *Catal. Today* 63 (2000) 397–404.
- [6] L.L. Murrel, R.T. Carlin, Silver on ceria: an example of a highly active surface phase oxide carbon oxidation catalyst, *J. Catal.* 159 (1996) 479–490.
- [7] P.W. Park, C.L. Boyer, Effect of  $\text{SO}_2$  on the activity of  $\text{Ag}/\gamma\text{-Al}_2\text{O}_3$  catalysts for NOx reduction in lean conditions, *Appl. Catal. B* 59 (2005) 27–34.
- [8] R. Brosius, K. Arve, M.H. Groothaert, J.A. Martens, Adsorption chemistry of NOx on  $\text{Ag}/\text{Al}_2\text{O}_3$  catalyst for selective catalytic reduction of NOx using hydrocarbons, *J. Catal.* 231 (2005) 344–353.
- [9] K. Villani, R. Brosius, J.A. Martens, Catalytic carbon oxidation over  $\text{Ag}/\text{Al}_2\text{O}_3$ , *J. Catal.* 236 (2005) 172–175.
- [10] A.E. Lavat, E.J. Baran, IR-spectroscopic characterization of  $\text{A}_2\text{BB}'\text{O}_6$  perovskites, *Vib. Spectrosc.* 32 (2003) 167–174.
- [11] S.D. Ross, *Inorganic Infrared and Raman Spectra*, McGraw-Hill Press, London, 1972.
- [12] N. Yamazoe, Y. Teraoka, Oxidation catalysis of perovskites—relationships to bulk structure and composition (valency, defect, etc.), *Catal. Today* 8 (1990) 175–199.
- [13] S. Ponce, M.A. Peña, J.L.G. Fierro, Surface properties and catalytic performance in methane combustion of Sr-substituted lanthanum manganites, *Appl. Catal. B* 24 (2000) 193–205.
- [14] R. Spinicci, A. Tofanari, Characterization of catalysts for methane-coupling by means of temperature programmed desorption, *Catal. Today* 6 (1990) 473–479.
- [15] S. Royer, F. Bérubé, S. Kaliaguine, Effect of the synthesis conditions on the redox and catalytic properties in oxidation reactions of  $\text{LaCo}_{1-x}\text{Fe}_x\text{O}_3$ , *Appl. Catal. A* 282 (2005) 273–284.
- [16] J.A.M. van Roosmalen, E.H.P. Cordfunke, R.B. Helmholdt, H.W. Zandbergen, The Defect Chemistry of  $\text{LaMnO}_{3\pm\delta}$ : 2. Structural Aspects of  $\text{LaMnO}_{3\pm\delta}$ , *J. Solid State Chem.* 110 (1994) 100–105.
- [17] S. Kaliaguine, A. Van Neste, V. Szabo, J.E. Gallot, M. Bassir, R. Muzychuk, Perovskite-type oxides synthesized by reactive grinding: Part I. Preparation and characterization, *Appl. Catal. A* 209 (2001) 345–358.
- [18] J. Liu, Z. Zhao, C. Xu, A. Duan, Simultaneous removal of NOx and diesel soot over nanometer Ln–Na–Cu–O perovskite-like complex oxide catalysts, *Appl. Catal. B* 78 (2008) 61–72.
- [19] S. Liu, A. Obuchi, J. Oi-Uchisawa, T. Nanba, S. Kushiya, An exploratory study of diesel soot oxidation with  $\text{NO}_2$  and  $\text{O}_2$  on supported metal oxide catalysts, *Appl. Catal. B* 37 (2002) 309–319.
- [20] J. Oi-Uchisawa, A. Obuchi, R. Enomoto, J. Xu, T. Nanba, S. Liu, S. Kushiya, Oxidation of carbon black over various  $\text{Pt}/\text{MO}_x/\text{SiC}$  catalysts, *Appl. Catal. B* 32 (2001) 257–268.
- [21] R. Burch, Knowledge and know-how in emission control for mobile applications, *Catal. Rev.* 46 (2004) 271–334.
- [22] J. Liu, Z. Zhao, J. Xu, A. Duan, G. Jiang, Q. Yang, The highly active catalysts of nanometric  $\text{CeO}_2$ -supported cobalt oxides for soot combustion, *Appl. Catal. B* 84 (2008) 185–195.
- [23] X. Bao, U. Wild, M. Muhler, B. Pettinger, R. Schlögl, G. Ertl, Co-adsorption of nitric oxide and oxygen on the  $\text{Ag}(110)$  surface, *Surf. Sci.* 425 (1999) 224–232.